HEAT TRANSFER OF AN IMPINGING JET - SENSITIVITY TOWARDS INFLOW CONDITIONS

F. Secchi, D. Gatti and B. Frohnapfel

Institute of Fluid Mechanics (ISTM), Karlsruhe Institute of Technology (KIT)

francesco.secchi@kit.edu

Abstract

The wall-heat transfer in the impingement region of a turbulent incompressible jet impinging onto a flat plate is assessed using direct numerical simulations. For impinging jets, the mean wall-heat transfer distribution along the plate features a global maximum close to the jet axis and, for specific configurations, a secondary peak further downstream of the impingement region. While the appearance of the latter maximum has been the focus of many investigations, the occurrence of the former and its links to the inflow conditions of the jet have only been alluded to by existing studies. The present research considers two different inflow conditions: a fully-developed turbulent pipe flow and a slightly convergent nozzle. The study shows that turbulent fluctuations, characterising the impingement region of the fully-developed turbulent inflow case, are significant in determining events of positive wall-heat transfer rates very close to the jet axis. On the contrary, similar events are not observed in the stagnation region of the convergent nozzle case, and the associated mean wall-heat transfer displays a markedly different distribution compared to the fully-developed turbulent inflow case.

1 Introduction

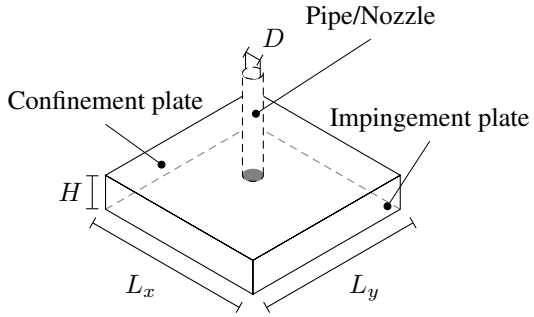

Figure 1: Computational domain and relevant geometrical parameters. The shaded area highlights the inflow section of the computational domain.

Jet impingement is a commonplace strategy exploited in technical applications to enhance the heat exchange close to a solid surface. Cooling turbine blades and electronic chips are, for instance, critical applications in which jet impingement plays a crucial role in keeping the integrity and correct functioning of the systems. Several experimental and numerical studies in the literature assess the heat transfer distribution along the impingement plate for a great span of parameters that define the flow configuration (Jambunathan et al., 1992; Viskanta, 1993). In general, the mean Nusselt number - defined as the ratio between convective to conductive heat transfer at the wall - is most sensitive to variations in nozzle-to-plate spacing, Reynolds number, inflow conditions at the nozzle exit section, and boundary conditions at the impingement wall. A non-monotonic decreasing behavior is observed for the Nusselt number along the plate, with an inner local maximum occurring within the impingement region (usually at $r \leq D/2$, where r indicates the radial distance from the jet axis and D the nozzle diameter) and, for certain parameter ranges, with a secondary peak located further away from the jet axis (typically at $r \approx 2D$). The presence of the latter peak is connected to flow structures that are primarily formed in the shear layer of the free jet and that are responsible for the formation of smaller scale vortical structures in the wall-jet region of the flow Dairay et al. (2015). This fact can be conveniently exploited for controlling the flow with the aim of increasing the overall wall-heat transfer. Nevertheless, the highest heat transfer rates are attained within the stagnation region of the flow, where the wall-directed fluid coming from the jet core is responsible for determining steep wall-normal gradients of temperature at the impingement plate. On top of this, turbulent fluctuations in the core of the jet are believed to determine an additional increase in the stagnation wall-heat transfer. The effects of turbulence on the stagnation wall-heat transfer of slot turbulent impinging jets were analysed experimentally by Gardon and Akfirat (1965). For nozzle-to-plate distances less than approximately $8B$ (B being the slot width) and for sufficiently large Reynolds numbers, the authors observed an increase in the mean stagnation wall-heat transfer with increasing nozzle-to-plate distance; a behavior that would not be expected since the centerline velocity of the jet remains very close to the centerline velocity at the nozzle section for such small nozzle-to-plate distances. As a consequence, a constant value for the stagnation wall-heat

transfer would be foreseen in the considered nozzle-to-plate range (Schrader, 1961). The observed increase in stagnation wall-heat transfer with increasing nozzle-to-plate distance was attributed by Gardon and Akfirat (1965) to the presence of intense turbulent fluctuations in the vicinity of the impingement plate. With increasing nozzle-to-plate spacing, turbulent fluctuations would become more intense due to a more effective mixing between the jet shear layer and the jet core and, along with that, an increase in stagnation wall-heat transfer could be expected (Corrsin, 1943). Nevertheless, this mechanism would soon become ineffective as a sufficiently large nozzle-to-plate distance were considered, for the corresponding decay of jet centerline velocity would overcome the beneficial effect of turbulent fluctuations on the stagnation wall-heat transfer. Since the early work of Gardon and Akfirat (1965), several studies have addressed the problem of characterizing the wall-heat transfer distribution in the stagnation region of impinging jets depending on the jet flow regime (Elison and Webb, 1994; Lee and Lee, 1999; Katti et al., 2011; Antošová and Trávníček, 2022). Such investigations address the problem experimentally with the main objective of determining correlations between the stagnation wall-heat transfer coefficient and Reynolds number and/or the nozzle-to-plate spacing. On the other hand, a more detailed investigation of the physical mechanisms governing the interplay between turbulence and the stagnation wall-heat transfer is not at hand yet. High-fidelity simulations, such as direct numerical simulations (DNS) or large eddy simulations (LES), are perfect candidates to help tighten this gap. Nonetheless, only a few numerical studies are currently available on the topic and the majority of them addresses the appearance of the secondary peak that characterizes the mean wall-heat transfer distribution along the impingement plate (Hadžiabdić and Hanjalić, 2008; Uddin et al., 2013; Dairay et al., 2015).

To further investigate the links between jet inflow conditions and the relevance of turbulent fluctuations on the stagnation region wall-heat transfer, we perform direct numerical simulations of an impinging jet issuing from a fully-developed turbulent pipe flow and a slightly convergent nozzle. Contrary to the fully-developed turbulent inflow, the latter is known to exhibit mild turbulent fluctuations in the jet core and to produce mean Nusselt number distributions featuring two distinct peaks away from the jet axis (Dairay et al., 2015; Viskanta, 1993).

2 Method of investigation

A jet issuing from either a fully-developed turbulent pipe flow or a convergent nozzle impinges orthogonally onto a plate placed at a distance $H = 2D$ away from the jet exit section. The Reynolds number, based on the nozzle diameter D and bulk mean velocity U_b, is $Re = 5300$. A sketch of the flow configuration is depicted in figure 1. The computational box has size $L_x = L_y = 8D$ in the x and y directions, respectively. For the chosen nozzle-to-plate distance and Reynolds number, it is expected for the stagnation wall-heat transfer to be affected by the presence of turbulent fluctuations near the vicinity of the wall. In addition, for such parameters, the DNS of the configuration remains accessible in terms of computational costs. In the simulations, two different Prandtl numbers of the fluid were considered, namely $Pr = 0.7$ and $Pr = 1$.

The divergence-free velocity and temperature fields are governed by the incompressible Navier-Stokes equations augmented with a transport diffusion equation for the temperature, which is treated as a passive scalar. Fully-developed inflow boundary conditions are enforced at the inlet section of the computational domain using a precursor simulation of a fully-developed turbulent pipe flow, whereas, for the convergent nozzle case, a top-hat mean velocity profile plus random sinusoidal fluctuations up to a cutoff azimuthal wave number are prescribed at the inlet section following the works of Tsubokura et al. (2003) and Dairay et al. (2015). Synthetic fluctuations are weighted in order not to excite the jet core. No-slip velocity boundary conditions are applied on both the impingement and confinement plates, whereas the energy-stable open-boundary conditions of Dong (2015) and Liu et al. (2020) are prescribed on the lateral surfaces of the domain for the velocity and temperature fields respectively. The impingement plate is kept at a constant and uniform temperature T_w and the confinement plate is considered at thermal equilibrium with the incoming jet flow at a temperature $T_j < T_w$. The governing equations are discretised in space on a Cartesian grid using the spectral element method (Maday and Patera, 1989). Time advancement is performed through an operator splitting procedure coupled with a third-order interpolation-extrapolation time integration scheme in which non-linear terms are treated explicitly and linear terms implicitly. The numerical method is implemented in the open-source flow solver `Nek5000` (Fisher et al., 2008-2020).

The computational box is discretised into $156 \times 156 \times 48$ elements in the x, y, and z directions, respectively. Wall-normal clustering of elements toward the impingement plate is used to better resolve the near-wall region. Stretching of elements is also applied in the x and y directions in order to cluster elements around the stagnation region of the flow. Results reported in this study refer to a 7^{th} polynomial degree solution and, hence, to a computational grid of the jet domain consisting of approximately $598 \cdot 10^6$ grid points.

3 Results

Mean axial velocity profiles scaled in wall units at the inflow section of the computational domain are dis-

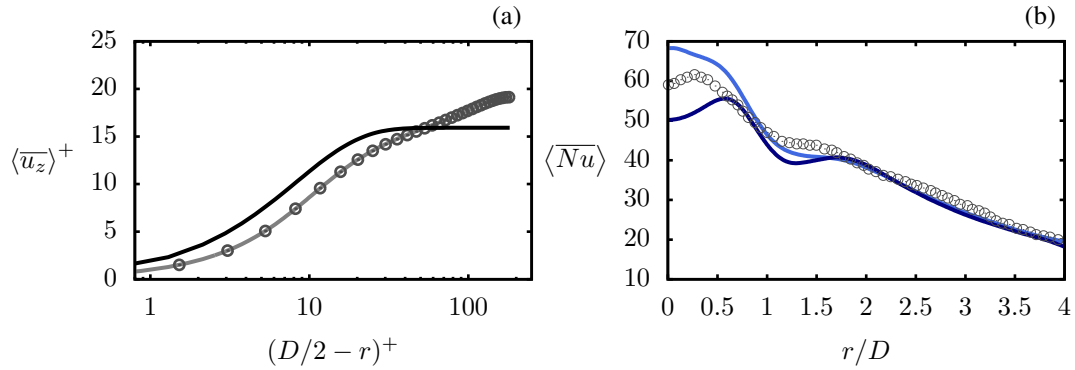

Figure 2: (a) Mean axial velocity profile at the jet exit section scaled in wall units as a function of the distance from the nozzle wall. Symbols are from Pirozzoli et al. (2021) and solid lines are from the present study. ——, fully-developed turbulent pipe flow; ——, convergent nozzle. (b) Mean Nusselt number distribution along the impingement plate for $Pr = 0.7$. Symbols are from Lee and Lee (1999); ——, convergent nozzle; ——, fully-developed turbulent inlet.

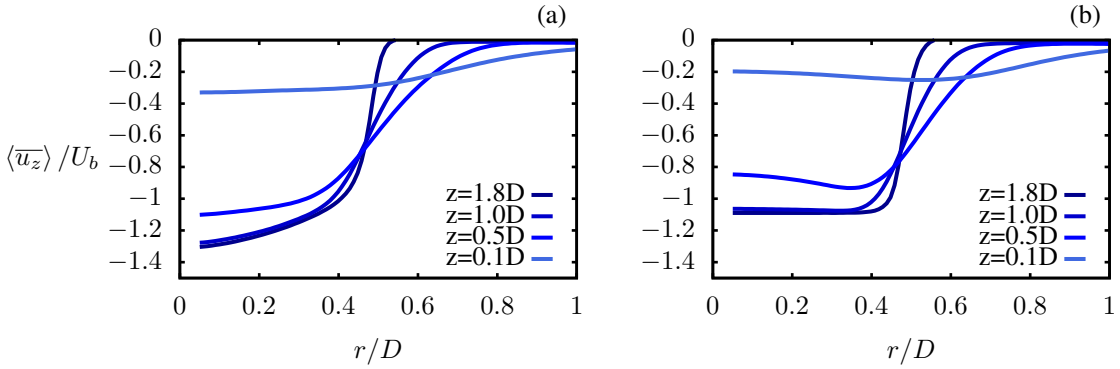

Figure 3: Jet mean axial velocity profiles at different wall-normal heights. (a) Fully-developed turbulent inflow; (b) Convergent nozzle.

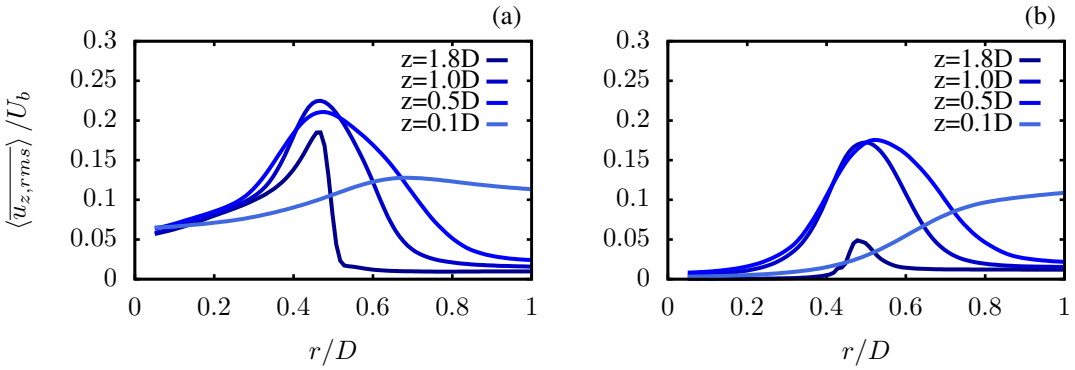

Figure 4: *R.m.s.* axial velocity fluctuations profiles at different wall-normal heights in the jet. (a) Fully-developed turbulent inflow; (b) Convergent nozzle.

played in figure 2a (scaling is indicated by a + superscript). For reference, the figure also reports data of a turbulent pipe flow at $Re_\tau = 180$ from Pirozzoli et al. (2021). In the figure and in what follows, the use of angle brackets and an overline indicates averaging in the circumferential direction and in time respectively. Statistics were collected in time for approximately 260 D/U_b. As a validation of the present data, figure 2b shows the mean Nusselt number distribution obtained in the present study compared to the experimental measurements of Lee and Lee (1999). The figure reports results for either jet inflow conditions and $Pr = 0.7$. The experimental data match very closely the present DNS results for a fully-developed turbulent inflow and Prandtl number 0.7 for radial distances greater than $D/2$. The agreement is substantially good also with the convergent nozzle data, as both inflow conditions result in very similar mean Nusselt number distributions in this region. At small radial distances, *i.e.* for $r < D/2$, the measured mean Nusselt number lies between the DNS data for both inflow conditions, perhaps indicating that the inflow attained during the experiment did not fully match either of the inflow conditions used in the DNS. In this respect, it

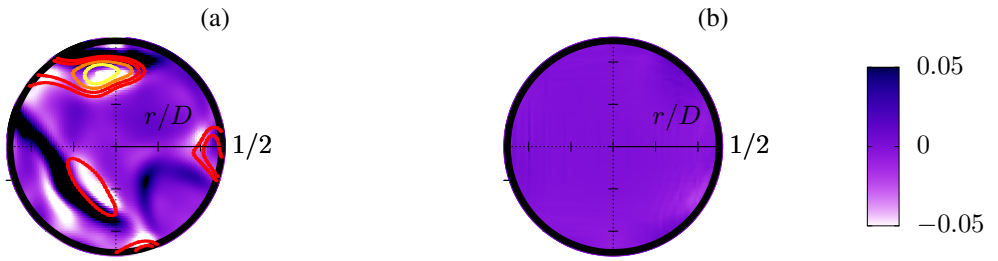

Figure 5: Instantaneous distribution of the wall-normal axial velocity gradient at the wall for $r \leq D/2$. Negative values indicate cold fluid directed toward the wall. (a) Fully-developed turbulent case; (b) convergent nozzle. Panel (a) also shows iso-contours of Nusselt number $Nu \geq 85$ at $Pr = 1$. The contours are color-coded from red to yellow in five equispaced levels ranging from 85 to 100.

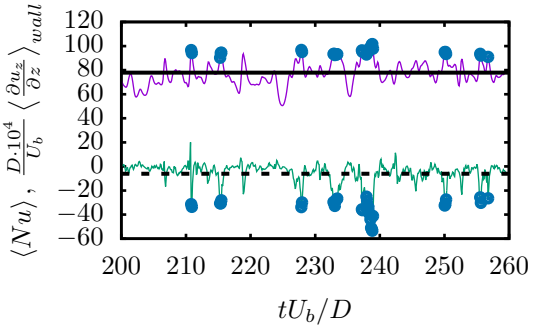

Figure 6: Time trace of the spatially averaged Nusselt number and wall-normal axial velocity gradient at the wall at $r = 0.05D$. To ease the visualization, the figure only depicts a portion of the total history of the simulation. Mean values are depicted by solid and black dashed lines, wherease symbols highlight peaks of Nusselt number and correspnding minima of the wall-normal axial velocity gradient at the wall.

should be noted that differences can also be attributed to slightly different Reynolds numbers and temperature wall boundary conditions (data from Lee and Lee (1999) is for $Re = 5000$ and fully Dirichlet boundary conditions for the temperature field are very difficult to achieve during an experiment). The effects of the investigated inflow conditions on the mean Nusselt number close to the jet axis are evident in the DNS data reported in figure 2b. The global maximum occurs in correspondence with the jet axis for the fully-developed turbulent case, whereas the convergent nozzle case shows a local minimum at the same location. The mean Nusselt number is sensibly greater in magnitude for the fully-developed turbulent inflow for radial distances $r < D/2$.

Large values of mean wall-heat transfer rates in the stagnation region are mainly determined by cold fluid coming from the bulk of the jet core. For this reason, it is instructive to observe the development of mean axial velocity profiles at different wall-normal distances for the two considered cases. This comparison is reported in figure 3. For the fully-developed turbulent inflow case (figure 3a), the mean axial velocity flattens as the jet moves closer to the impingement plate, but its radial development remains monotonically decreasing with the global minimum occurring at the center-line of the jet. On the contrary, for the convergent nozzle case, the mean axial velocity readily develops a minimum in the axial velocity profile away from the center-line of the jet (figure 3b). In both cases, close to the wall, the location of the minimum mean axial velocity corresponds to the location of the global peak of the Nusselt number observed in figure 2b. This observation qualitatively confirms that, in the stagnation region, very large wall-heat transfer rates are achieved due to the jet core which is responsible for bringing, on average, cold fluid very close to the impingement plate. Nevertheless, for the fully-developed turbulent inflow case, an effect of turbulent fluctuations on the stagnation region mean wall-heat transfer could be expected. As it can be seen in figure 4, root-mean-square (*r.m.s.*) axial velocity fluctuations close to the jet center-line tend to decay very slowly along the jet axis for the fully-developed turbulent inflow case (figure 4a). Even further, for the same case, turbulent fluctuations appear to slightly increase in the vicinity of the jet center-line while moving towards the impingement plate (*e.g.* curve at $z/D = 0.1$). On the other hand, for the convergent nozzle case (figure 4b), axial velocity fluctuations appear to maintain a very small magnitude for $r/D < 2$ at every examined wall-normal location. The presence of significant axial velocity fluctuations near the impingement plate could affect the local heat transfer rate. In particular, sweep events of cold fluid directed towards the hot wall would produce a local steepening of the wall-normal temperature gradient. Such a scenario is expected to occur to a much less extent, if at all, for the convergent nozzle case where turbulent fluctuations occur mainly in the shear layer of the jet, whereas in the jet core, they are much weaker compared to the fully-developed turbulent case. This speculation gains support by observing the two instantaneous snapshots of the wall-normal gradient of the axial velocity component distribution at the impingement wall reported in figure 5. Negative values of this quantity identify near-wall regions

of wall-directed fluid. As it can be seen in figure 5a, these regions correlate very well with occurrences of large positive fluctuations of Nusselt number (these are displayed by contour lines in the figure). On the other hand, figure 5b shows that similar events have a much weaker intensity for the convergent nozzle case and, correspondingly, their influence on Nusselt number fluctuations is expected to be marginal. Because of this observation, the analysis of the statistical relevance of the occurrence of such events on the stagnation mean wall-heat transfer is reported in the following only for the fully-developed turbulent inflow case. The time history of the spatially averaged Nusselt number and wall-normal axial velocity gradient at the wall at $r = 0.05D$ are reported in figure 6. The figure only depicts a portion of the total time history to ease the visualization; further, the wall-normal axial velocity gradient is magnified in the figure by a factor of 10^4 to allow the comparison with the Nusselt number signal. The figure evidences the good correlation occurring between events of very large Nusselt number and bursts phenomena characterized by largely negative wall-normal axial velocity gradients. To assess the statistical relevance of such events, the joint probability density function (PDF) of Nusselt number and wall-normal axial velocity gradient at the wall at $r = 0.05D$ is shown in figure 7. The skewed shape of

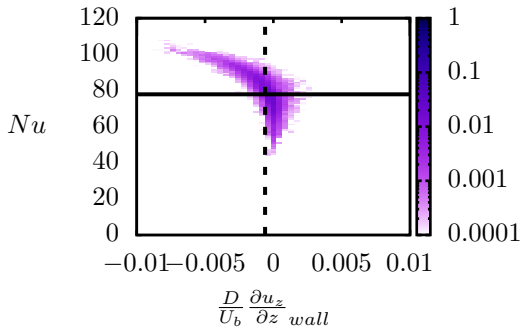

Figure 7: Joint PDF of Nusselt number and wall-normal axial velocity gradient at the wall at $r = 0.05D$. Mean values are depicted by solid and black dashed lines.

the joint-PDF observed in the figure results from the occurrence of intermittent events of very large positive fluctuations of Nusselt number which take place concurrently with wall-directed axial velocity fluctuations. To have an estimate of the actual relevance of turbulent fluctuations on the mean wall-heat transfer, the Nusselt number along the impingement plate is averaged conditionally by excluding events for which the wall-normal axial velocity gradient at the wall is less than $-0.00265U_b/D$. The arbitrary choice of this value was assumed upon the analysis of the joint PDF of figure 7. The resulting conditional average is compared to the non-conditional average of the Nusselt number distribution in figure 8 for the fully-developed turbulent inflow case and in figure 9 for the convergent nozzle case. The figures underline the regions along the impingement plate where turbulent fluctuations produce a net impact on the mean wall-heat transfer. For the fully-developed turbulent inflow case, these are the stagnation region (*i.e.* $r < 0.5D$ approximately) and, similar to the findings of Dairay et al. (2015), the region around the secondary peak at approximately $r = 2D$. On the other hand, because of the absence of significant turbulent fluctuation in the stagnation region of the convergent nozzle case, the stagnation region wall-heat transfer is not affected by conditional averaging.

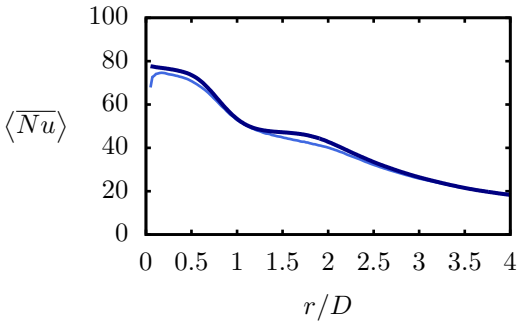

Figure 8: Mean Nusselt number distribution along the impingement plate for $Pr = 1.0$. Fully-developed turbulent inflow case. ——, conditional average with $\frac{\partial u_z}{\partial z}_{wall} > -0.00265U_b/D$; ——, unconditional average.

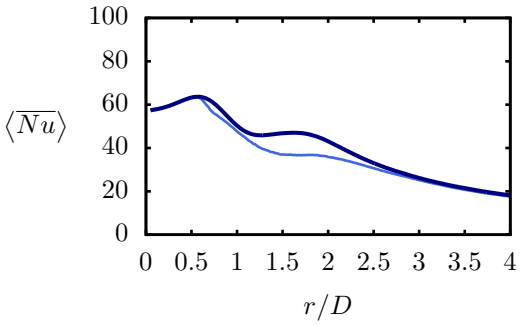

Figure 9: Mean Nusselt number distribution along the impingement plate for $Pr = 1.0$. Convergent nozzle inflow case. ——, conditional average with $\frac{\partial u_z}{\partial z}_{wall} > -0.00265U_b/D$; ——, unconditional average.

4 Conclusions

The present study investigated the wall-heat transfer associated with turbulent impinging jets originating from a fully-developed turbulent pipe flow and a convergent nozzle. The Reynolds number, based on the pipe diameter D and mean bulk velocity U_b, was $Re = 5300$ and the nozzle-to-plate spacing was $2D$. For the investigated configuration, results in the lit-

erature indicate a significant dependence of the mean wall-heat transfer on turbulent fluctuations close to the wall with the major impact taking place in the stagnation region (Gardon and Akfirat, 1965; Elison and Webb, 1994; Lee and Lee, 1999; Katti et al., 2011; Antošová and Trávníček, 2022) and in the region close to the location of the secondary peak in the mean Nusselt number distribution (Hadžiabdić and Hanjalić, 2008; Uddin et al., 2013; Dairay et al., 2015). While the connection between the unsteady flow field and the local mean wall-heat transfer near the secondary Nusselt number peak region has been intensively investigated in the past, much less attention has been given in the literature to the heat transfer in the stagnation region. Using direct numerical simulation, the present work has shown the links bonding turbulent fluctuations coming from the jet core with the stagnation region mean wall-heat transfer. In particular, it is shown that intermittent events of cold wall-directed fluid are responsible for producing intense peaks of very large wall-heat transfer rates near the jet axis. The occurrence of such events determines a highly skewed joint probability density function of Nusselt number and wall-normal axial velocity gradient at the wall in the stagnation region of the jet. By conditional averaging, it was shown how the mean Nusselt number distribution along the impingement plate is modified when intermittent events of high wall-heat transfer rates are excluded from the averaging process.

Acknowledgments

We greatly acknowledge the support by the German Research Foundation (DFG) under the Collaborative Research Centre TRR150 (project number 237267381). The simulations presented in this work were performed on the HPE Apollo (Hawk) supercomputer at the High Performance Computing Center Stuttgart (HLRS) under the grant number zzz44198.

References

Z. Antošová and Z. Trávníček. Stagnation Point Heat Transfer to an Axisymmetric Impinging Jet at Transition to Turbulence. *ASME J. of Heat and Mass Transfer*, 145(2):023902, 2022. ISSN 2832-8450.

S. Corrsin. Investigation of flow in an axially symmetrical heated jet of air. Technical report, 1943.

T. Dairay, V. Fortuné, E. Lamballais, and L.-E. Brizzi. Direct numerical simulation of a turbulent jet impinging on a heated wall. *J. of Fluid Mech.*, 764: 362–394, 2015.

S. Dong. A convective-like energy-stable open boundary condition for simulations of incompressible flows. *J. Comput. Phys.*, 302:300 – 328, 2015.

B. Elison and B.W. Webb. Local heat transfer to impinging liquid jets in the initially laminar, transitional, and turbulent regimes. *Int. J. of Heat and Mass Transfer*, 37(8):1207–1216, 1994. ISSN 0017-9310.

P.F. Fisher, J.W. Lottes, and S.G. Kerkemeier. NEK5000 Version 19.0. `https://nek5000.mcs.anl.gov/`, 2008-2020. Argonne National Laboratory, Illinois.

R. Gardon and J.C. Akfirat. The role of turbulence in determining the heat-transfer characteristics of impinging jets. *Int. J. of Heat and Mass Transfer*, 8 (10):1261–1272, 1965. ISSN 0017-9310.

M. Hadžiabdić and K. Hanjalić. Vortical structures and heat transfer in a round impinging jet. *J. of Fluid Mech.*, 596:221–260, 2008.

K. Jambunathan, E. Lai, M.A. Moss, and B.L. Button. A review of heat transfer data for single circular jet impingement. *Int. J. of Heat and Fluid Flow*, 13(2): 106–115, 1992.

Vadiraj V. Katti, S. Nagesh Yasaswy, and S. V. Prabhu. Local heat transfer distribution between smooth flat surface and impinging air jet from a circular nozzle at low reynolds numbers. *Heat and Mass Transfer*, 47(3):237–244, 2011. ISSN 1432-1181.

J. Lee and S. J. Lee. Stagnation region heat transfer of a turbulent axisymmetric jet impingement. *Exp. Heat Transfer*, 12(2):137–156, 1999.

X. Liu, Z. Xie, and S. Dong. On a simple and effective thermal open boundary condition for convective heat transfer problems. *Int. J. of Heat and Mass Transfer*, 151:119355, 2020.

Y. Maday and A.T. Patera. Spectral element methods for the incompressible Navier-Stokes equations. In *State of the art surveys on computational mechanics ASME*, pages 71–143, 1989.

S. Pirozzoli, J. Romero, M. Fatica, R. Verzicco, and P. Orlandi. One-point statistics for turbulent pipe flow up to $Re_\tau \approx 6000$. *J. of Fluid Mech.*, 926:A28, 2021.

H. Schrader. *Trocknung feuchter Oberflächen mittels Warmluftstrahlen: Strömungsvorgänge und Stoffübertragung*. VDI-Verlag, 1961.

M. Tsubokura, T. Kobayashi, N. Taniguchi, and W.P. Jones. A numerical study on the eddy structures of impinging jets excited at the inlet. *Int. J. of Heat and Fluid Flow*, 24(4):500–511, 2003.

N. Uddin, S.O Neumann, and B. Weigand. LES simulations of an impinging jet: On the origin of the second peak in the nusselt number distribution. *Int. J. of Heat and Mass Transfer*, 57:356–368, 2013. ISSN 0017-9310.

R. Viskanta. Heat transfer to impinging isothermal gas and flame jets. *Exp. Thermal and Fluid Science*, 6 (2):111–134, 1993.